

Introduction

With advancements in Carbon-fiber reinforced plastics (CFRP) structures, the development of high-performance gliders has led to a continuous growth of the aspect ratio and the span. Modern sailplanes with a span of 25 m have aspect ratios of more than forty, while maximum achieved span is over thirty meters and ratios of more than fifty, achieve significant reductions in induced drag.

The aerodynamic gain of large spans is in conflict with other design criteria for the overall optimization of gliders. The ability of making agile turns when entering thermals is essential for the overall performance of a sailplane (that includes climb and cruise segments). Unfortunately the agility of a light aircraft with an enormous wingspan is poor due to its moment of inertia. In addition, the adverse yaw, which is produced by the application of the ailerons, rises with the span and significantly deteriorates both the controllability and the performance of the sailplane. Performance weaknesses are caused by an increased area of the vertical tail which is necessary to overcome the adverse yaw.

Various methods are applied to support the vertical tail in neutralizing the negative moment around the vertical axis were passive systems (which are usually required for sailplanes). These methods are based on two distinct principles. One reduces the amount of the adverse yaw (e.g. differential ailerons), while another counteracts it or compensates for it (e.g. (jet-) spoilers). These methods have the disadvantages of producing low roll rates and too much drag, respectively. The potential of a passive tip blow-out system that is sketched in Figs. 1 and 2 as a non-drag based system has been evaluated in this paper to overcome the adverse yaw.

Design requirements

Changing the path of a flow means changing its momentum with respect to the related directions. If the flow is directed through a tube with an elbow, the course of the flow will be changed by ninety degree (cf. Fig. 1 and 2). In such a situation the x component of momentum will be changed from $m \cdot v_x$ to zero. Following the second law of Newton, the rate of change of the momentum leads to a force on the wall of the elbow in that direction. At the same time the momentum in the y-direction is changed from zero to $m \cdot v_y$, which results in a force in the y-direction. When only one elbow is taken in consideration, the resulting force in x-direction can be interpreted as a drag while the force in y-direction can be taken as a transverse force.

Two elbows in a tube system can be used to change the direction of the flow twice such that the final direction is the same as the original inlet direction (x-direction). The resulting forces generate a pair of transverse forces that result in a strain of the pipe and its mount and a moment around the vertical axis as shown in Fig. 3. In the case of a constant cross-sectional tube system, the force on the elbow wall in the x-direction is affected by the velocity of the flow, the cross sec-

tional area and the total pressure loss of the system. The pressure loss is affected by the length of the cylindrical system and the efficiency of the elbows. On the other hand, the resulting yaw moment also is affected by the lever arm of the two elbows where the forces are generated. That lever should be the longest part of the tube system which leads spanwise through the wing. Because most friction of the system is produced in that part, there is an optimum lever of the whole system compromising friction loss and lever arm of the moment. Thus, the design of the internal flow system is mainly driven by the span, the air speed and the cross sectional area, which should be as large as possible.

When a duct system is installed as an internal flow system, a constant cross sectional tube should be preferred because the weight of the system is small and the pressure loss is low compared to other cross sections due to the maximum ratio of volume and tube surface and minimal secondary flow effects. Unfortunately, the diameter of the tube is limited by the available thickness of the wing which usually varies along the span. Therefore, the diameter of the tube is restricted by the dimensions of the outer wing. High performance sailplanes have thicknesses of about 0.03 m to 0.05 m at the tip. For such aircraft, it can be appropriate to change the cross section of the tube along the span using variable diameter or different shapes.

Design procedure

An internal flow system was designed to compensate the adverse yaw. The flow system is initially assumed to be a constant cross-sectional tube system, as shown in Fig. 3. It consists of an inlet, two elbows, a spanwise connection of the elbows and an outlet. The position of the inlet can either be close to the nose of the fuselage or in the wing leading edge. The exact position depends on the desired distance between the two elbows.

The adverse yaw is assumed to be mainly caused by the asymmetric induced drag distribution of a wing with deflected ailerons. Thus, estimates were made using the lifting-line theory and a numerical solution according to Multhopp¹. The lifting-line theory is applicable for un-swept wings and provides valid results for sailplanes. Since the adverse yaw should be compensated before the glider starts to roll, roll-damping effects are neglected. In addition, the estimation of the adverse yaw without taking the roll damping effect into account is more conservative, because it would lower the adverse yaw.

Calculation of internal flow system

The mechanical model of the tube system is shown in Fig. 4. Following the principle of linear momentum for a stream filament² the resulting force of the momentum is described in Eq. (1).

$$\underline{F}_m = \int_{s_1}^{s_2} \frac{\partial(\dot{m} \cdot \underline{e})}{\partial t} \cdot ds + \dot{m}_2 \cdot v_2 \cdot \underline{e}_2 - \dot{m}_1 \cdot v_1 \cdot \underline{e}_1 \quad (1)$$

Assumptions were made that the stream is steady state with constant mass flow. Following the principle of “action et reaction”, the force on the wall in x-direction of the outer elbow (cf. Fig 4) can be calculated as follows:

$$\underline{R}_{w_3}^x = [\dot{m} \cdot v_3 + (p_3 - p_\infty) \cdot A_3] \cdot \underline{e}_3 \quad (2)$$

As it can be seen in Eq. 2, the forces that generate the moment are affected by the static pressure at the outlet. That pressure is decreased due to the installation of mounting parts (e.g. inlet, elbows or nozzles) and the friction of the flow in the tube system.

The resulting total pressure loss of the system can be calculated according to Eq. 3.

$$\Delta p_L = \rho \cdot \lambda \cdot \frac{L}{D} \cdot \frac{v^2}{2} + \rho \cdot \sum_k \zeta_k \cdot \frac{v_k^2}{2} \quad (3)$$

The friction is impacted by the relative length of the tube, the fluid density, the velocity of the flow and the friction coefficient which is Reynolds number dependent. The empiric approach of Prandtl and v. Karman⁴ was used to estimate the friction coefficient for turbulent tube flow using Eq. 4.

$$\lambda = \frac{0.309}{[\log(\text{Re}/7)]^2} \quad (4)$$

The second part of the sum in Eq. 3 considers the pressure losses of a number of k installed mounting parts which can be found in Ref. 1 and Ref. 4. In accordance with the described method, the internal flow and its forces on the wall of the cylinder were calculated. Finally, the force on the wall including the pressure losses can be calculated using Eq. 5.

$$\underline{R}_{w_3}^x = [\dot{m} \cdot v - \Delta p_L \cdot A_1] \cdot \underline{e}_3 \quad (5)$$

Estimation of the adverse yaw

Ailerons are deflected to locally increase or reduce the camber of the airfoil. The resulting asymmetrical lift distribution will roll the aircraft. An example lift coefficient distribution with deflected ailerons is shown in Fig. 5. Simultaneously, an asymmetric induced drag distribution will yaw the aircraft contrary to the desired turn direction. Large span sailplanes begin to yaw before starting to roll because of their big moment of inertia around the longitudinal axis and the roll damping effect. The induced drag distribution is taken to be the key reason for adverse yaw while the influence of an asymmetrical profile drag distribution was neglected. Usually gliders have wings with high aspect ratios ($AR > 6$) and no sweep. Therefore, the simple lifting-line theory of Prandtl is applicable for

lift distribution calculations³ where the geometrical, the effective and the induced angle of attack are related as shown in Eq. 6.

$$\alpha_g(y) = \alpha_e(y) + \alpha_i(y) \quad (6)$$

The lifting-line theory must be extended when the influence of ailerons is to be taken into account. An appropriate approach can be found in Ref. 3, where an additional local angle of attack due to aileron deflection is added just to the geometrical angle of attack as shown in Eq. 7, and the additional angle can be calculated using Eq. 8 and Eq. 9 with the deflection angle of the ailerons.

$$\alpha(y) = \alpha_g(y) + \alpha_a(y) \quad (7)$$

$$\alpha_a = \alpha_{\eta a} \cdot \xi \quad (8)$$

$$\alpha_{\eta a} = -\frac{2}{\pi} \cdot \left[\sqrt{\lambda_a} \cdot (1 - \lambda_a) + \arcsin(\sqrt{\lambda_a}) \right] \quad (9)$$

The term λ_a in Eq. (9) is the relative length of the aileron l_a/l . The specific circulation distribution can be calculated using the aspect ratio, the relative aileron length and span, the aileron deflection angle, the geometrical angle of attack of the wing, the free-stream velocity and the density. With the resulting circulation distribution, the drag coefficient distribution can be calculated using Eq. 10.

$$c_{d_i}(y) = AR \cdot \gamma(y) \cdot \alpha_i(y) \quad (10)$$

The result is shown in Fig. 6 in combination with the lift coefficient distribution and the distribution of the geometrical angle of attack. The adverse yaw coefficient c_{N_ξ} is the integral of the local drag coefficients multiplied with the respective lever to the centerline of the airplane. The adverse yaw can be calculated from the coefficient c_{N_ξ} and the span, as stated in Eq. 11, where the wing area can be calculated from the aspect ratio and the span. This leads to Eq. 12.

$$N_\xi = c_{N_\xi} \cdot \frac{\rho}{2} \cdot v^2 \cdot A_{\text{wing}} \cdot \frac{b}{2} \quad (11)$$

$$N_\xi = c_{N_\xi} \cdot \frac{\rho}{4} \cdot v^2 \cdot \frac{b^3}{AR} \quad (12)$$

For a sailplane having the following characteristics:

- Span $b = 25$ m,
- Aspect ratio $AR = 40$,
- Angle of attack $\alpha = 2^\circ$,
- Relative aileron chord length $\lambda_a = 0.2$,
- Relative aileron span $b_a/b = 0.4$,
- Aileron deflection angle $\xi = 5^\circ$,
- Air speed $v_\infty = 70$ knots

The adverse yaw calculated with the method mentioned above turns out to be approximately 91 N·m.

Experimental procedure

To verify the design procedure, a tube system consisting two elbows was tested in an in-house free-stream wind tunnel. Because of the two elbows, the tube system tested has a Z shape as displayed in Figs. 3 and 4. Only the inlet of the tube system is blown by the free-stream since the inlet of an equivalent system which is integrated within a wing also is the sole part which is attacked by the air flow.

Wind tunnel and model

The free-stream wind tunnel is shown in Fig. 7. It has a circular outlet at the end of the nozzle with a diameter of 5 cm. The maximum free-stream speed is about 150 km/h. Before the model was blown by the wind tunnel, the dynamic pressure was measured using a Prandtl tube to calibrate the actual velocity of the flow. The model tube system has a diameter of 1.3 cm which is small compared to the nozzle outlet to ensure a relative homogeneous velocity distribution along its inlet area. The moment generated by the air flowing outside of the tube has a damping effect. It is negligible small due to its insignificant lever arm to the bearing. Two different lengths of the cross tube were used to validate the influence of the moment lever and the length of the tube system. One length was 0.25 m while the other was 0.5 m.

Experimental methods

The tube system was mounted on a bearing on the first elbow. On the second elbow a spring balance was installed to measure the force on the wall of the tube in x-direction as shown in Fig. 8. The speed of the blower was controlled using a ring transformer. The voltage for a certain speed can be read out from the connected voltmeter to calibrate the measured dynamic pressure with respect to the adjusted voltage. The speed-dependent moment was determined by multiplying the measured force on the spring balance with the lever of the cross tube.

Experimental results

As mentioned above, measurements of the moment around the vertical axis were made using a tube system model and a free stream wind tunnel for different flow speeds. The result of the speed-dependent moment is presented in Fig. 9 where the lever is 0.25 m. In Fig. 10, the result of the measurements with the lever of 0.5 m is shown. In addition, the theoretical curves calculated using Eq. 5 also are displayed in the respective diagram for comparison. It can be observed that the theoretical results are close to the measurements. Especially the speed-dependent trend is covered extremely well. Since the actual values of the installation loss coefficients were unknown, the slightly too high level of the theoretical results is mainly caused by the assumption of a too optimistic inlet loss

coefficient of 0.85 for the theoretical analysis. The noticeable kink in the distributions is caused by a change of hardware during the experiment since the measuring range of the spring balances was smaller than the imposed range of forces on it. Therefore, they needed to be substituted having minor differences in their calibration.

Comparison of internal-flow-system and adverse-yaw-estimation results

To answer the initial question of the potential of a yaw moment generation using a wing-internal-flow system, the experimental results were compared to the adverse yaw calculation (Eq. 12). For the aircraft described above, the adverse yaw was determined to be 91 N·m. The influence of the diameter and the lever to the generated moment is presented in Fig. 11. It can be seen that the achievable moment produced by the tube system increases with both the lever (i.e. span) and the diameter of the tube. The influence of the diameter turns out to be progressive. Assuming that the lever is equal to the span of the aircraft, it becomes perceptible that a diameter of 8.4 cm is necessary to generate a moment of 91 N·m (cf. Fig. 11). In case of space-limiting airfoil thicknesses, either the diameter has to be reduced or the cross section can be varied span-wise. If the relative thickness of the wing tip allows only a tube diameter of 4 cm, the adverse yaw can be only reduced by 21%.

When looking to Fig. 12, the contrary character of increasing the lever for relatively small diameters becomes observable. It can be seen that the optimum lever is 12.5 m for a tube system having a constant diameter of 1 cm. Furthermore, the produced moment is about 0.36 N·m.

Predicting the drag produced by the system while generating the yaw moment needs further investigations, which is not done yet. Nevertheless, a pessimistic estimation can be made by simply multiplying the total pressure loss and the constant cross sectional area given as part of Eq. 5. This estimation leads to a drag of the tube system of about 5 N. However, when the pressure loss is equal or greater than the dynamic pressure of the free stream, the duct is virtually closed. No air will flow through the tube and no yaw moment is generated. Since there is air in the tube, a virtual stagnation pressure will become apparent and the shape of the streamlines will be similar to a wing section without an uncovered inlet. It becomes obvious, that the wing profile drag will not increase by the product of the dynamic pressure and the circular area of the inlet. A hole in the leading edge of a wing section that leads to a dead end zone will have a minor influence to the wing profile drag. To some extent that condition is comparable to one of the pitot tube.

The drag of the vertical stabilizer, when it is used to compensate the adverse yaw, is mainly based on the induced drag of the VTP. Assuming a lever arm of the VTP of 5m, a force is 18.2 N is necessary to fully compensate adverse yaw of the above mentioned example (adverse yaw of 91 N·m). From the

given data of the example and a realistic size of the VTP, the induced drag is around 0.06 N. This value is considerably less than the pessimistic estimation of the tube internal drag. To answer the question whether or not having a drag advantage in the short-time, turn-entering phase, a more detailed drag calculation has to be done for the duct system including the actual configuration and construction of the inlet.

This drag advantage also has a big influence on the performance during straight flight. Under ideal conditions, both the inlet and the outlet will not lead to any drag increase during straight flight. That can be achieved primarily by a good smooth covering of the inlet. Therefore, without more detailed investigations and specific construction solutions a final benchmark of the overall performance cannot be provided.

Concluding remarks

A wing-internal-flow system was identified to counteract the adverse yaw of high performance sailplanes when the entire span is used. Even when some drag is generated, this system is not drag-based and has good potential in overall performance enhancement of gliders: the vertical tail may be sized smaller not having the task to compensate for the adverse yaw. If the rudder can be eliminated, as a consequence of the different way of yaw moment generation, the weight of the sailplane will be reduced and the wetted area will be smaller. Besides the direct weight reduction due to the absence of the rudder, the load cases of the fuselage can be reduced by the bending moment and the torque of a deflected rudder. Therefore, another weight reduction can be achieved. In addition, there would be less induced drag of the vertical stabilizer. Assuming that the inlet is covered when it's not in use, the overall profile drag will be lower in straight flight. In comparison to the drag generated by the vertical-tail-plane, the drag of the tube system is free from induced drag. Performance calculations, including the trade-off between drag reduction and weight increase (or decrease), will be investigated as a next step.

The calculations are based on a tube system that is characterized by having a constant circular cross section. That approach is limited by the available thickness of the wing tip. As it was shown in Fig. 11, the diameter (i.e. cross sectional area) via the mass flow has an enormous impact to the generated moment. Therefore, leading the air flow cross-wise through the wing (e.g. between the leading edge and the spar) without installing an additional duct seems to be the best solution as long as the direction of the flow is changed twice and the related losses are moderate. When designing the internal flow system, it has to be kept in mind that for small cross-sectional areas the optimum distance between inlet and outlet can be smaller than the wing span. In general, if the area is greater than a circular cross section with a diameter of 2 cm, both inlet and outlet should be located at the wing tip to maximize the lever arm and, hence, the moment. As a consequence, the configuration shown in Fig. 1 is not preferable since the result-

ing lever arm is much below the optimum combination of lever arm and cross sectional area.

The results are considered preliminary because:

1. Predicting the drag produced by the system while generating the yaw moment needs further investigation.
2. A more detailed drag calculation has to be done for the duct system including the actual configuration and construction of the inlet.
3. Without more detailed investigations and specific construction solutions, a final benchmark of the overall performance cannot be provided.

Finally, to be more confident that this yaw control method is sufficiently described and to provide further validation of the results, a free flight technology demonstrator using the tip blow-out system for yaw control is currently built. This demonstrator is a scale glider with a span of 4 m. The results of related flight tests will be presented at OSTIV XXX.

References

- ¹Multhopp, H., *Die Berechnung der Auftriebsverteilung von Tragflügeln*, Luftf.-Forschg., page 153-169, 1938.
- ²Siekamnn, H.E., *Strömungslehre*, Springer-Verlag, Berlin, 2000.
- ³Schlichting, H., Truckenbrodt, E., *Aerodynamik des Flugzeuges* Bd.2, Springer-Verlag, Berlin, 1960.
- ⁴Beitz, W., Grote, K.-H., *Dubbel – taschenbuch für den Maschinenbau*, Springer-Verlag, Berlin, 2001.

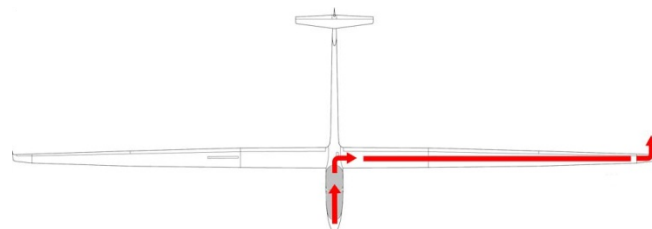


Figure 1 Path of air flow through a semi span covered internal flow system in a typical high-performance sailplane.

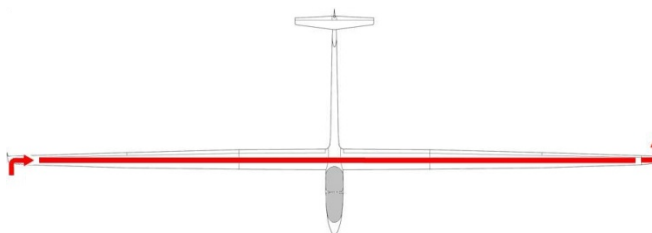


Figure 2 Path of air flow through a complete span covered internal flow system in a typical high-performance sailplane.

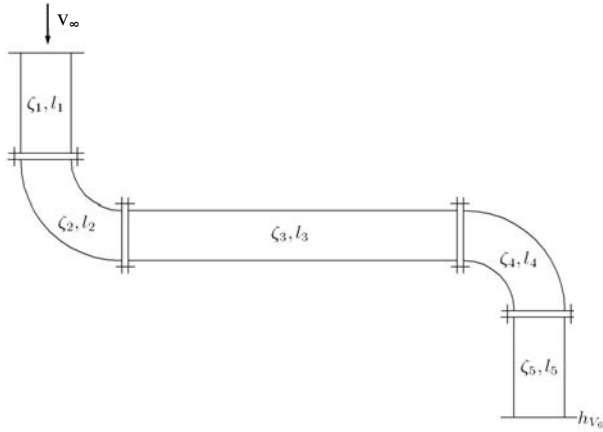


Figure 3 Constant cross sectional tube system as internal flow system.

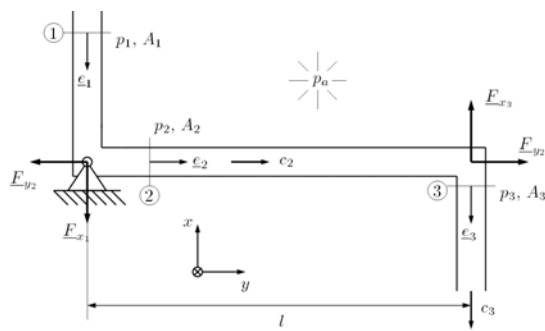


Figure 4 Mechanical model of the semi span covered tube system.

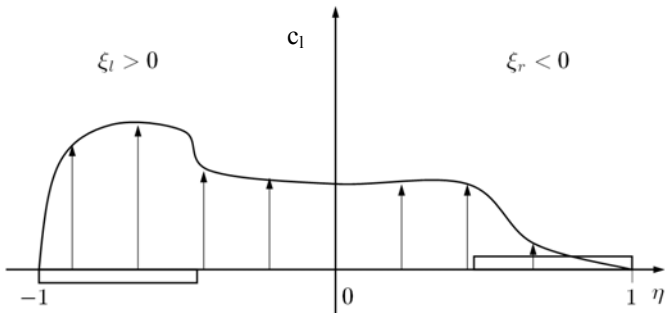


Figure 5 Example of lift coefficient distribution with deflected ailerons.

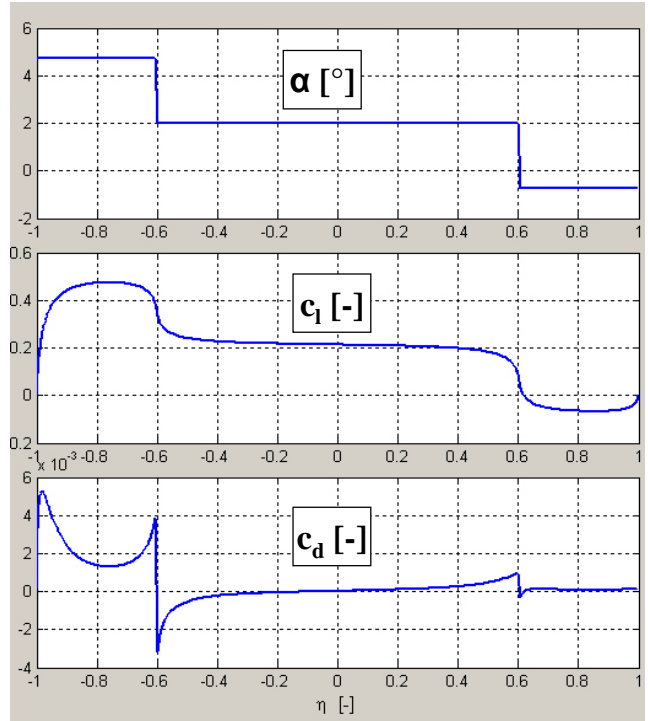


Figure 6 Distributions of local angle of attack, local lift coefficient, and local drag coefficient.



Figure 7 Small free-stream wind tunnel of TU Berlin.

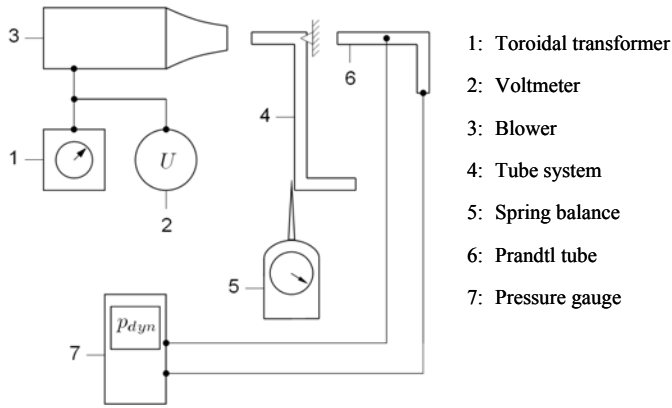


Figure 8 Experimental setup.

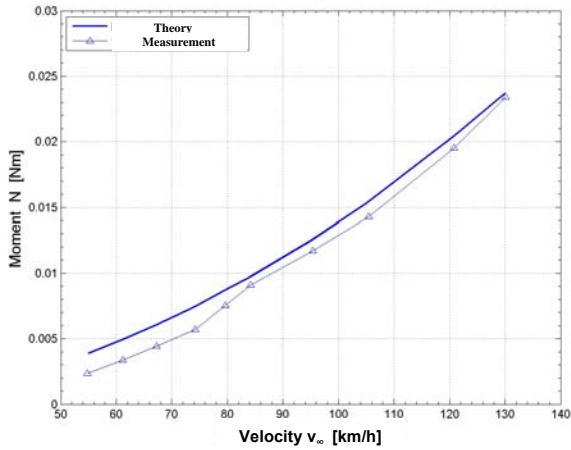


Figure 9 Comparison of theoretical and measured results (lever arm length of 0.25 m).

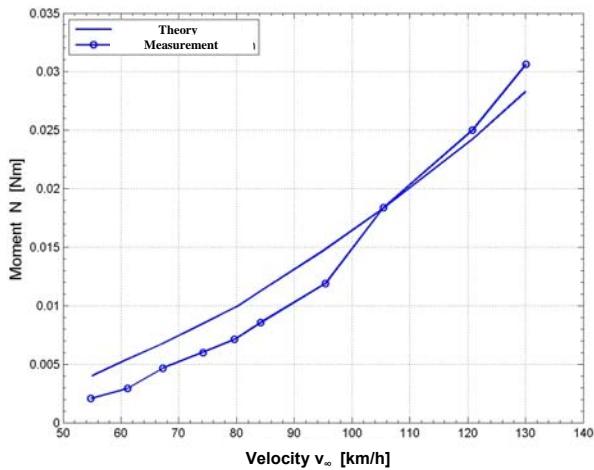


Figure 10 Comparison of theoretical and measured results (lever arm length of 0.5 m).

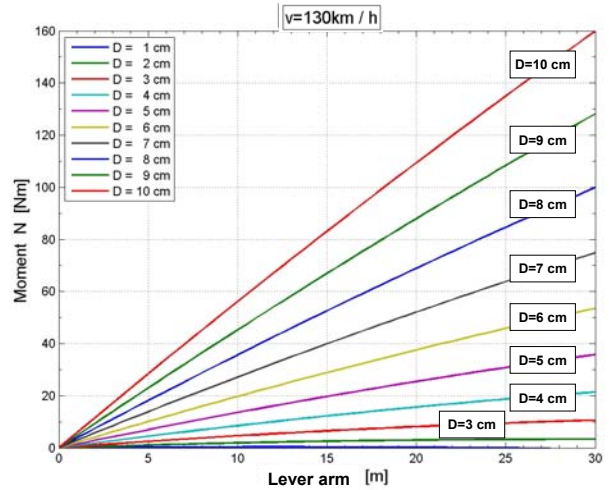


Figure 11 Influence of diameter and lever arm on yaw moment ($D = 1 \text{ cm} - 10 \text{ cm}$).

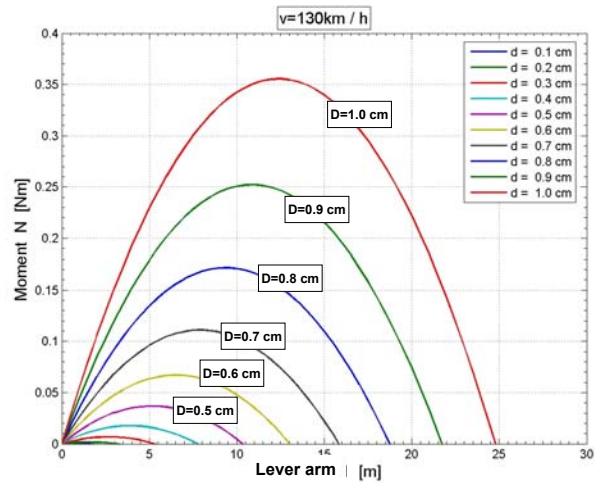


Figure 12 Influence of diameter and lever arm on yaw moment ($D = 0.1 \text{ cm} - 1.0 \text{ cm}$).